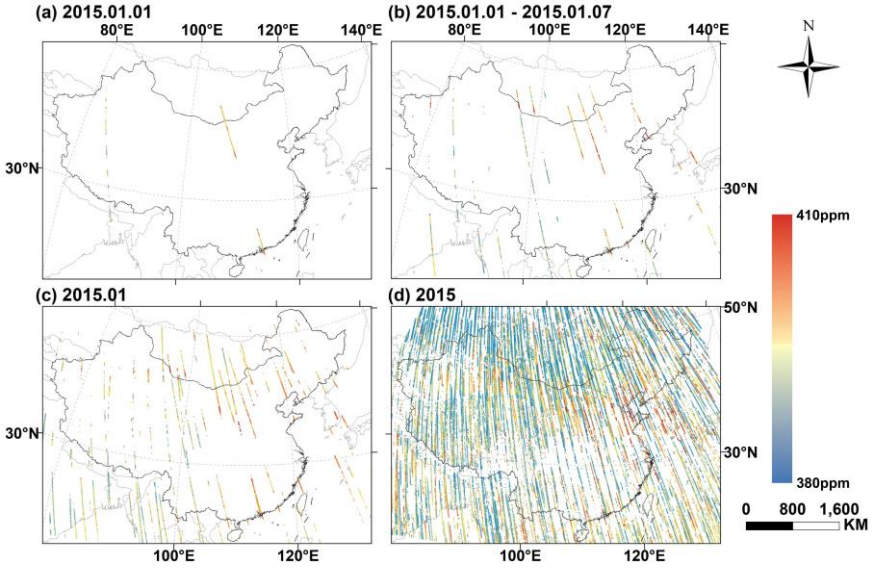

Figure S1. The XCO2 data acquired by OCO-2 at daily, weekly, monthly, and yearly time scales.

Table S1. ERA5 variables collected in this study.

Short name	Units	Description
blh	m	It is the depth of air next to the Earth's surface which is most affected by the resistance to the transfer of momentum, heat or moisture across the surface. The boundary layer height calculation is based on the bulk Richardson number (a measure of the atmospheric conditions) following the conclusions of a 2012 review.
u10	m s^{-1}	It is the horizontal speed of air moving towards the east, at a height of ten meters above the surface of the Earth.
v10	m s^{-1}	It is the horizontal speed of air moving towards the north, at a height of ten meters above the surface of the Earth.
si10	m s^{-1}	It is the horizontal speed of the wind, or movement of air, at a height of ten meters above the surface of the Earth.
msl	Pa	This parameter is the pressure (force per unit area) of the atmosphere at the surface of the Earth, adjusted to the height of mean sea level.
t2m	K	It is the temperature of air at 2m above the surface of land, sea or inland waters.
E	m of water equivalent	This parameter is the accumulated amount of water that has evaporated from the Earth's surface, including a simplified representation of transpiration (from vegetation), into vapour in the air above.
skt	K	This parameter is the temperature of the surface of the Earth.
ssr	J m^{-2}	This parameter is the amount of solar radiation that reaches a horizontal plane at the surface of the Earth minus the amount reflected by the Earth's surface.
sp	Pa	This parameter is the pressure (force per unit area) of the atmosphere at the surface of land, sea and inland water.
tco3	kg m^{-2}	This parameter is the total amount of ozone in a column of air extending from the surface of the Earth to the top of the atmosphere.
tcw	kg m^{-2}	This parameter is the sum of water vapour, liquid water, cloud ice, rain and snow in a column extending from the surface of the Earth to the top of the atmosphere.
tp	m	This parameter is the accumulated liquid and frozen water, comprising rain and snow, that falls to the Earth's surface. It is the sum of large-scale precipitation and convective precipitation.
totalx	K	This parameter gives an indication of the probability of occurrence of a thunderstorm and its severity by using the vertical gradient of temperature and humidity.

Table S2. EGG4 variables collected in this study.

Short name	Units	Description
aco2gpp	kg m^{-2}	Accumulated CO_2 Gross Primary Production
aco2nee	kg m^{-2}	Accumulated CO_2 Net Ecosystem Exchange
aco2rec	kg m^{-2}	Accumulated CO_2 Ecosystem Respiration
fco2gpp	kg m^{-2} s^{-1}	Flux of CO_2 Gross Primary Production
fco2nee	kg m^{-2} s^{-1}	Flux of CO_2 Net Ecosystem Exchange
fco2rec	kg m^{-2} s^{-1}	Flux of CO_2 Ecosystem Respiration
tcch4	ppb	CH_4 column-mean molar fraction
tcco2	ppm	CO_2 column-mean molar fraction

Section S1. Spatiotemporal stationarity and testing methods

Firstly, Exploratory Data Analysis (EDA) was used to examine the normality of the residuals. As evident from the histogram in Figure S2, the residuals approximately obeyed a normal distribution, which means the CNN model has the ability to capture the primary trends and relationships within the data, affirming the rationality and effectiveness of utilizing the CNN model.

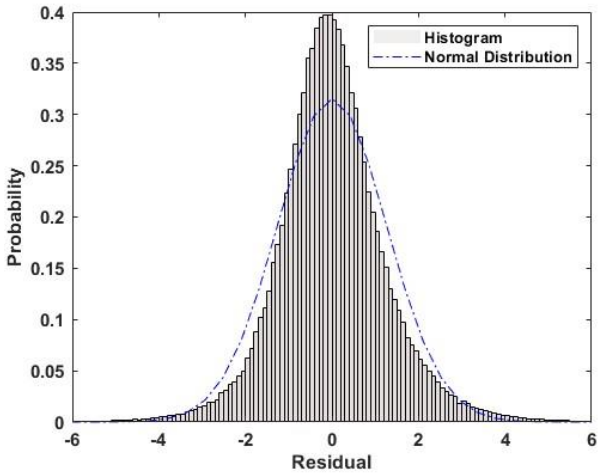

Figure S2. Histogram of residual frequency distribution of CNN model

Secondly, the Augmented Dickey-Fuller test (ADF test) was used to validate the assumption of stationarity for the residuals. ADF test is an evolution of Dickey-Fuller test (DF test), which was proposed by Dickey and Fuller in 1979 as a method to test whether the time series data satisfies the assumption of stationarity [1,2]. The test is based on whether the time series data contains a unit root. If there is a unit root in the time series data, it is non-stationary; conversely, if there is no unit root, the time series data is stationary. The null hypothesis of the ADF test is H_0: $\delta = 0$, and the alternative hypothesis is H_1: $\delta < 0$. In other words, the null hypothesis posits the existence of a unit root, indicating non-stationarity, while the alternative hypothesis suggests the absence of a unit root and the potential inclusion of a constant and time trend, indicating stationarity in the data. The t-statistic is defined as $T_\rho = \frac{\delta}{\sigma_\rho}$, where δ represents the parameter of the regression model estimated through the least squares method, and σ_ρ is the standard deviation estimate of ρ. If $T_\rho \geq$ the critical value, the null hypothesis H_0 is accepted, indicating non-stationarity in the data. In contrast, if $T_\rho <$ the critical value, the null hypothesis H_0 is rejected, signifying stationarity in the data. Additionally, consideration should be given to whether the p-value is less than the significance level. The ADF test results are presented in Table S3.

Table S3. ADF test results.

		T-Statistic	P-Value
Augmented Dickey-Fuller test statistic		-5.3912	0.0000
Test critical values	1% level	-3.5274	
	5% level	-2.9038	
	10% level	-2.5893	

From the ADF test results, it can be seen that the p-value is 0.0000, which is less than 1%. The t-statistic is -5.3912, falling below the critical values of -3.5274, -2.9038, and -2.5893 for the 1%, 5%, and 10% significance levels, respectively. This proves the null hypothesis is rejected at the 1% confidence level, affirming that the time series data is stationary.

Section S2 Spatiotemporal Kriging: Sample variogram function and theoretical variogram function

The construction of the variogram involves two steps: calculating the sample variogram function and selecting an appropriate theoretical model along with parameter estimation [3]. According to the observed data points at finite locations $Z(X_1), Z(X_2), \cdots, Z(X_n)$, the sample variogram function is calculated by the following formula (Equation (1)) [4]:

$$\gamma^*(h) = \frac{1}{2N(h)} \sum_{i=1}^{N(h)} [Z(x_i + h) - Z(x_i)]^2 \quad (1)$$

Where $\gamma^*(h)$ represents the sample variogram function, $N(h)$ denotes the number of pairs of sample points. h represents a discretized measure, also known as the lag distance. Based on the distribution of the scatter plot of the sample variogram function, this study chose the exponential model (Equation (2)) as the theoretical model and used the least squares method for parameter estimation [4].

$$\gamma(h) = \begin{cases} 0, & h = 0 \\ C_0 + C_1 \left(1 - e^{-\frac{h}{a}}\right), & h \neq 0 \end{cases} \quad (2)$$

Where C_0 represents the nugget effect, C_1 denotes the partial sill, $(C_0 + C_1)$ corresponds to the sill, and $3a$ is the range. The fitted spatial empirical variogram function and temporal empirical variogram function of the residuals are illustrated in Figure S3. Both functions exhibit a satisfactory fit to the residual distribution, with a fitting error MSE ranging from 0.001 to 0.008. The corresponding parameters are detailed in Table S4. The product-sum model is used to fit the empirical spatiotemporal variogram function, and the fitting error MSE is 0.009. As depicted in Figure S4, it is evident that the fitted theoretical variogram function achieves a relatively stable spatiotemporal sill within certain temporal and spatial distances.

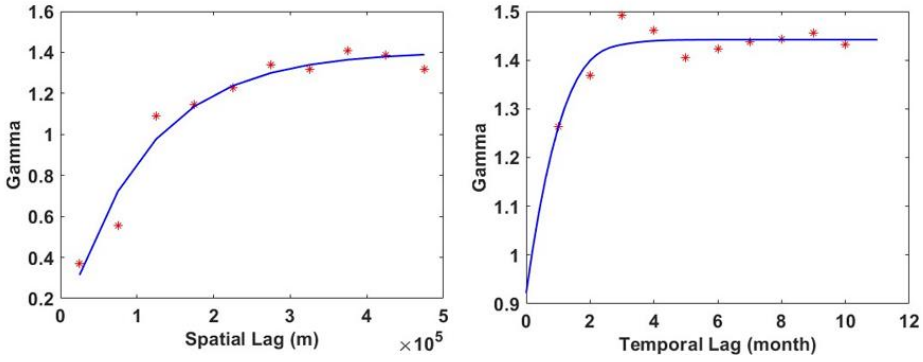

Figure S3. The spatial empirical variogram function and temporal empirical variogram function of the residuals (red points), and their corresponding fitted variogram function models (blue lines).

Table S4. The optimal parameters of the theoretical spatiotemporal variogram function model.

	Nugget	Patial sill	Range
Space	0.0268	1.3787	320650.3986 (m)
Time	0.6822	0.7599	2.0939 (month)

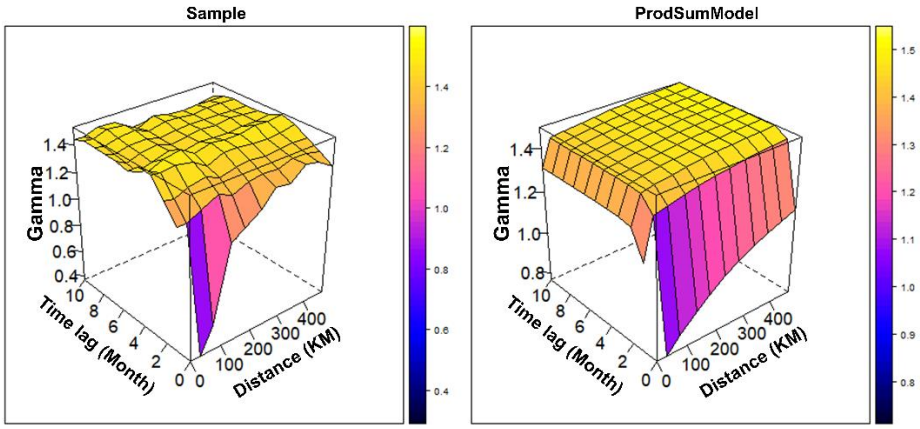

Figure S4. The empirical spatiotemporal variogram functions for residuals and its fitted variogram function model.

Section S3. Wilcoxon signed-rank test

Non-parametric statistical tests were performed for CNN-STK XCO2 and CAMS XCO2 using the Wilcoxon signed-rank test. The P-values indicate the probability of observing the test statistic or a more extreme value under the null hypothesis. If the P-value below the standard significance level (typically 0.05), the null hypothesis can be rejected, indicating a significant difference between the two datasets at the given significance level. Meanwhile, the result of the hypothesis test (H) is a logistic value, indicating whether the null hypothesis is rejected. If H equals 1, the null hypothesis is rejected; if H equals 0, the null hypothesis is not rejected. Stats contains additional statistical information about the test.

The test result of the two datasets in this experiment is shown in Table S5. It can be observed that the P-value in each period is less than 0.01 and the H-value is 1, indicating a significant difference between CNN-STK XCO2 and CAMS XCO2 data at a 1% significance level.

Table S5. Non-parametric statistical test results for CNN-STK XCO2 and CAMS XCO2.

Month	P-value	H	Stats
Jan-15	5.8415E-290	1	402956040.5
Feb-15	2.5446E-208	1	391775740.5
Mar-15	6.44156E-42	1	357305507
Apr-15	7.45431E-08	1	319487748
May-15	5.0618E-307	1	255405572.5
Jun-15	0	1	125008195
Jul-15	0	1	82329358.5
Aug-15	0	1	90171766.5
Sep-15	0	1	59273910
Oct-15	4.80418E-24	1	350459786
Nov-15	0	1	501921987.5
Dec-15	0	1	450872049
Jan-16	0	1	429148956
Feb-16	0	1	448260328.5
Mar-16	0	1	449332336
Apr-16	0	1	424109692
May-16	1.18431E-71	1	294461455
Jun-16	0	1	174931941.5
Jul-16	0	1	133018527
Aug-16	0	1	111566521

Sep-16	1.27672E-82	1	291766695
Oct-16	0	1	536735901.5
Nov-16	0	1	564730218
Dec-16	0	1	566284209.5
Jan-17	0	1	541211648
Feb-17	0	1	558612567
Mar-17	0	1	560768016.5
Apr-17	0	1	547160913
May-17	4.6005E-176	1	386876874.5
Jun-17	0	1	195135459
Jul-17	0	1	187370692.5
Aug-17	0	1	211227748.5
Sep-17	4.66944E-11	1	343319169.5
Oct-17	0	1	572274156.5
Nov-17	0	1	619937503.5
Dec-17	0	1	602294972
Jan-18	0	1	558560001.5
Feb-18	0	1	542843735
Mar-18	0	1	615051869
Apr-18	0	1	554066404.5
May-18	4.2923E-132	1	379208450.5
Jun-18	0	1	184110872
Jul-18	0	1	145371459.5
Aug-18	0	1	172492512.5
Sep-18	5.55451E-16	1	346448326.5
Oct-18	0	1	561752037.5
Nov-18	0	1	612312562.5
Dec-18	0	1	600875774.5
Jan-19	0	1	574854598.5
Feb-19	0	1	557194036
Mar-19	0	1	569865249
Apr-19	0	1	465647911
May-19	1.29603E-06	1	320495796
Jun-19	0	1	149211619.5
Jul-19	0	1	74632821
Aug-19	0	1	45421999
Sep-19	0	1	14396731
Oct-19	0	1	92656523.5
Nov-19	0	1	168127811.5
Dec-19	0	1	183751694
Jan-20	0	1	178075429.5
Feb-20	0	1	174083114
Mar-20	0	1	198514838.5
Apr-20	0	1	102225706.5
May-20	0	1	94038235
Jun-20	0	1	11417122
Jul-20	0	1	22792072.5
Aug-20	0	1	12647360
Sep-20	0	1	1017501

Oct-20	0	1	9564130.5
Nov-20	0	1	20960281.5
Dec-20	0	1	50451431.5

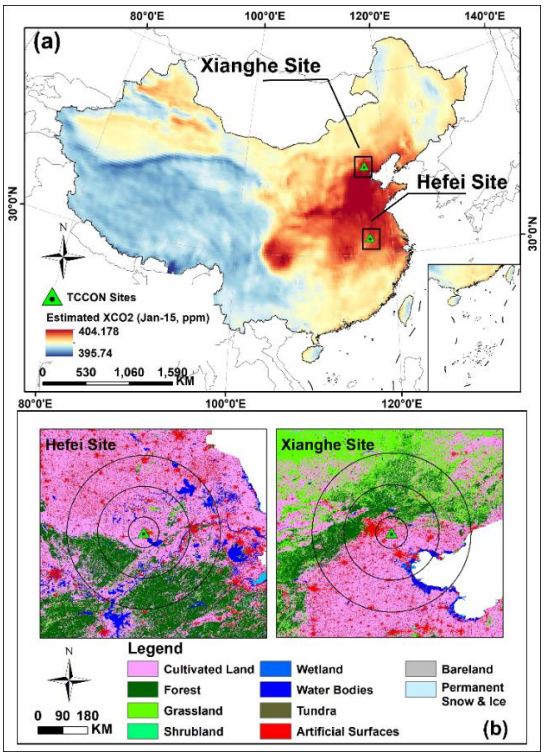

Figure S5. Locations of Hefei site and Xianghe site (a). Circular geographical regions centered on each site, with diameters of 1°, 3°, and 5°. The land cover data was obtained from GlobeLand30 dataset (http://globallandcover.com/ (accessed on 9 November 2023)), and the blank area in the diagrams is the oceanic area (b).

Section S4 Results of high and low values clustering

We initially used the Global Moran's I to assess the spatial autocorrelation of atmospheric CO_2 concentration within the study area, with values ranging from -1 to 1. A smaller P-value (typically less than 0.05) rejects the null hypothesis. Here, when Moran's I is greater than 0, the data exhibit positive spatial correlation, while Moran's I less than 0 indicates a negative correlation, and a value of 0 signifies no correlation. A Z-score > 1.65 suggests clustered distribution of data, while a Z-score < -1.65 indicates dispersed distribution; otherwise, the data are considered randomly distributed. We computed the Global Moran's I for four seasons, with results presented in Table S6.

Table S6. Global Moran's I of different seasons.

	Spring	Summer	Autumn	Winter
Global Moran's I	0.979	0.998	0.978	0.980
Z score	224.585	228.837	224.276	224.859
P value	0.000	0.000	0.000	0.000
Pattern	Clustered	Clustered	Clustered	Clustered

Next, we utilized the Optimized Hot Spot Analysis method to further identify statistically significant clusters of high and low values within the study area. This method is based on the Local Getis-Ord Gi* statistic, which uses Z-scores and P-values to identify locations where high or low values cluster spatially. A locality is considered a statistically significant hotspot if it contains a high value surrounded by other high values; conversely, it is classified as a cold spot. The Local Getis-Ord Gi* can be expressed as Equation (3) [5].

$$G_i^* = \frac{\sum_{j=1}^{n} \omega_{i,j} x_j - \bar{X} \sum_{j=1}^{n} \omega_{i,j}}{S \sqrt{\frac{\left[n \sum_{j=1}^{n} \omega_{i,j}^2 - \left(\sum_{j=1}^{n} \omega_{i,j} \right)^2 \right]}{n-1}}} \quad (3)$$

Where, x_j is the attribute value of element j, $\omega_{i,j}$ is the spatial weight between element i and j, n is the total number of elements, and:

$$\bar{X} = \frac{\sum_{j=1}^{n} x_j}{n} \quad (4)$$

$$S = \sqrt{\frac{\sum_{j=1}^{n} x_j^2}{n} - (\bar{X})^2} \quad (5)$$

G_i^* statistics are Z scores, so no further calculations are needed. Finally, the distribution of XCO2 cold and hot spots in different seasons is shown in Figure S6.

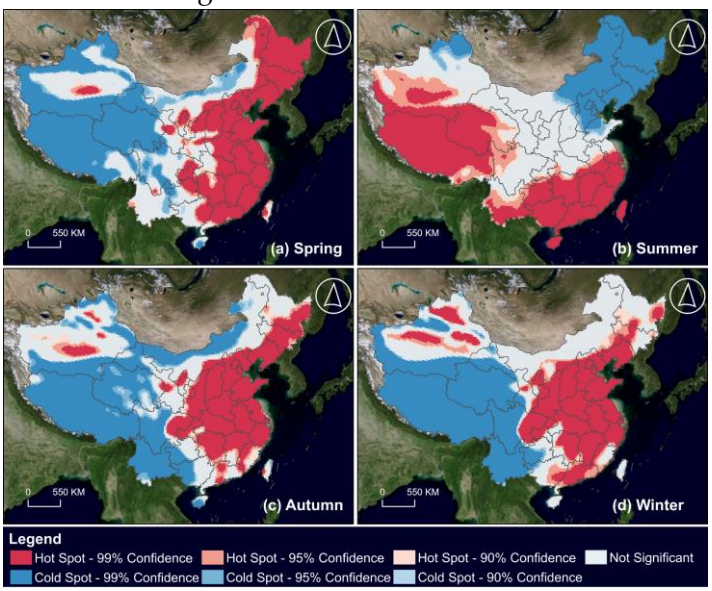

Figure S6. Spatial distribution of hot and cold spots of XCO2 in different seasons.

Reference

1. Worden, K.; Iakovidis, I.; Cross, E.J. New Results for the ADF Statistic in Nonstationary Signal Analysis with a View towards Structural Health Monitoring. *Mech. Syst. Signal Process.* **2021**, *146*, 106979, doi:10.1016/j.ymssp.2020.106979.
2. Gianfreda, A.; Maranzano, P.; Parisio, L.; Pelagatti, M. Testing for Integration and Cointegration When Time Series Are Observed with Noise. *Econ. Model.* **2023**, *125*, 106352, doi:10.1016/j.econmod.2023.106352.
3. Varouchakis, E.A.; Hristopulos, D.T. Comparison of Spatiotemporal Variogram Functions Based on a Sparse Dataset of Groundwater Level Variations. *Spat. Stat.* **2019**, *34*, 100245, doi:10.1016/j.spasta.2017.07.003.
4. Sukkuea, A.; Heednacram, A. Prediction on Spatial Elevation Using Improved Kriging Algorithms: An Application in Environmental Management. *Expert Syst. Appl.* **2022**, *207*, 117971, doi:10.1016/j.eswa.2022.117971.
5. Getis, A.; Ord, J.K. The Analysis of Spatial Association by Use of Distance Statistics. *Geogr. Anal.* **1992**, *24*, 189–206, doi:10.1111/j.1538-4632.1992.tb00261.x.